SENRA Academic Publishers, Burnaby, British Columbia
Vol. 4, No. 3, pp. 1303-1309, October 2010
Online ISSN: 1920-3853; Print ISSN: 1715-9997

Canadian Journal of pure&applied sciences

CHARACTERIZATION OF ZnO NANOPOWDERS SYNTHESIZED BY THE DIRECT PRECIPITATION METHOD

*HK Farag[1], Z M Hanafi[1], M Dawy[2] and EM Abd El Aziz[1]
[1]Inorganic Chemistry Department, National Research Centre, Dokki, Cairo
[2]Physical Chemistry Department, National Research Centre, Dokki, Cairo, Egypt.

ABSTRACT

The present paper deals with the synthesis of zinc oxide nanoparticles via a direct precipitation method using zinc acetate dihydrate as a precursor. The synthesized ZnO powder was characterized by means of XRD, UV-Visible and IR spectroscopy, SEM-EDX and TG-DTA. The XRD results reveal that the synthesized ZnO has the wurtzite phase structure with a crystallite size of about 50nm. The ZnO particles are spherical in shape and only zinc and oxygen were detected by EDX analysis signifying the high purity of the synthesized ZnO. The UV-Vis. spectrum of the ZnO powder indicates a band gap of about 3.2 eV, showing a slight red shift compared to the band gap of the bulk ZnO (3.37 eV). The prepared ZnO powder exhibits a specific surface area of 16.5 m^2 g^{-1}, determined by Brunauer-Emmett-Teller (BET) equation.

Keywords: Zinc oxide, direct precipitation, characterization, band gap.

INTRODUCTION

In recent times, wide bandgap semiconductor oxides such as ZnO, TiO_2 or SnO_2 have attracted extensive attention due to their wide range of technological applications including gas sensing, photocatalysis, piezoelectricity and optoelectronics (Carotta *et al*., 2005). Among semiconductor oxides ZnO has found much interest. Its high gas sensitivity and chemical stability make ZnO a potential candidate for gas sensing (Martins *et al*., 2004 and Carotta *et al*., 2009). The wide band gap of ZnO (3.37 eV) as well as its high exciton binding energy (60 meV) promote its application as light emitting or laser diodes (Alivov *et al*., 2003). ZnO nanorodes have been characterized for the application as hydrogen gas sensors (Wang *et al*., 2005). Jiaquiang *et al*. (2005) have reported the gas sensing properties of ZnO nanorodes. ZnO powders have successfully been employed as electrode materials for dye-sensitized solar cells (DSSCs) as an alternative to TiO_2 (Redmond *et al*., 1994). Furthermore, nanocrystalline ZnO is generally used in cosmatics because of its ability to protect from ultraviolet rays and its capability to kill and restrain bacterium (Deng *et al*., 2001).

There are several methods for synthesis of ZnO via solution based processes such as, e.g., sol-gel (Gao *et al*., 2007; Rani *et al*., 2008), hydrothermal (Xu *et al*., 2004), direct precipitation (Sigoli *et al*., 1997, Music *et al*., 2002 ; Bitenc *et al*., 2008) and electrochemical routes (Nyffenegger *et al*., 1998). Direct precipitation from aqueous solutions of zinc salts, such as $ZnCl_2$, $ZnSO_4$, $ZnNO_3$, in presence of ammonium carbonate or urea is a widely used method for synthesis of nanostructured ZnO. This method involves the precipitation of zinc hydroxyl carbonate (basic zinc carbonate) precursors which transform to ZnO via thermal decomposition at temperatures above 300^{o}C.

In the present paper we have employed the direct precipitation method to synthesize nanocrystalline ZnO by using zinc acetate dihydrate as a precursor. Different microscopic and spectroscopic techniques were used to characterize the synthesized ZnO powder, such as scanning electron microscopy with energy dispersive X-ray (SEM-EDX), X-ray diffraction (XRD), infrared (IR), ultraviolet-visible (UV-vis.), thermogravimetric (TG) and differential thermal analysis TG-DTA. The surface area of the ZnO powder was determined by BET (Brunauer-Emmett-Teller) measurements.

MATERIALS AND METHODS

EXPERIMENTAL

Zinc acetate dihydrate (Aldrich, 99.99 %) and anhydrous ammonium carbonate (Alfa 99.99%) were used without further purification as the starting materials for the synthesis of ZnO. Distilled water was used to prepare the precursor solutions. Sodium hydroxide (Sigma-Aldrich 98%) was used to adjust the pH.

The phase compositions of the prepared powder were analyzed by X-ray diffraction (XRD) using a Siemens D-5000 diffractometer with CoK_α radiation. The morphology and composition of the obtained ZnO powder were investigated by means of a high resolution field emission scanning electron microscope (Carl Zeiss DSM

*Corresponding author email: msherif888@yahoo.com

982 Gemini) and energy dispersive X-ray analyzer. UV/Vis absorption spectrum was recorded on a Hewlett-Packard 8452A diode array spectrophotometer. The IR spectrum was recorded using a Bruker-Vector 22 spectrometer. The KBr pellet technique with about 1 wt. % of sample was used for sample preparation.

Thermal gravimetric (TG) and differential thermal analysis (DTA) were carried out by a NETZSCH STA 409 PC thermal analyzer at a heating rate of 10 °C /min. starting from room temperature up to 700°C in air. Nitrogen sorption results were obtained using a Quantachrome Autosorb-1 automated gas sorption analyser. Prior to sorption measurements, the sample was degassed for 6 hours at 150°C under pressure of 100 μTorr. The surface area was calculated by the BET (Brunauer-Emmett-Teller) equation.

RESULTS AND DISCUSSION

Synthesis of ZnO nanoparticles

The nanocrystalline ZnO powder was prepared using $Zn(CH_3COO)_2.2H_2O$ and anhydrous $(NH_4)_2CO_3$ as starting materials by a direct precipitation method. Appropriate amounts of both $Zn(CH_3COO)_2.2H_2O$ and $(NH_4)_2CO_3$ were separately dissolved in 100mL distilled water to prepare 0.5M and 1M solutions, respectively. Then the two solutions were carefully mixed under continuous stirring and then heated at 60°C for 3 hours to complete the reaction. A white precipitate of basic zinc carbonate was the reaction product. The resulting precipitate was filtered and washed several times with distilled water. Afterwards, the obtained precipitate was calcined at 450°C for 3 hours. The calcination was carried out in order to thermally decompose the formed basic zinc carbonate to ZnO.

Characterization of the synthesized ZnO

XRD and SEM-EDX

The XRD pattern of the synthesized ZnO powder is shown in figure 1. It is clearly seen that ZnO is highly crystalline and all diffraction peaks are well indexed to the diffraction pattern of wurtzite phase of ZnO (JCPDS 36-1451). The inset of figure 1 shows the broadening of the main diffraction peaks, (100), (002) and (101). As seen the recorded peaks are broad indicating the small crystallite size of the synthesized ZnO. The average crystallite size of ZnO was estimated according to Scherrer's equation (Scherrer 1918):

$$d = 0.9\lambda / \beta_{1/2} \cos\theta \qquad (1)$$

where, d is the crystallite size, λ the X-ray wavelength (1.7889 Å for CoKα), $\beta_{1/2}$ the full-width half maximum

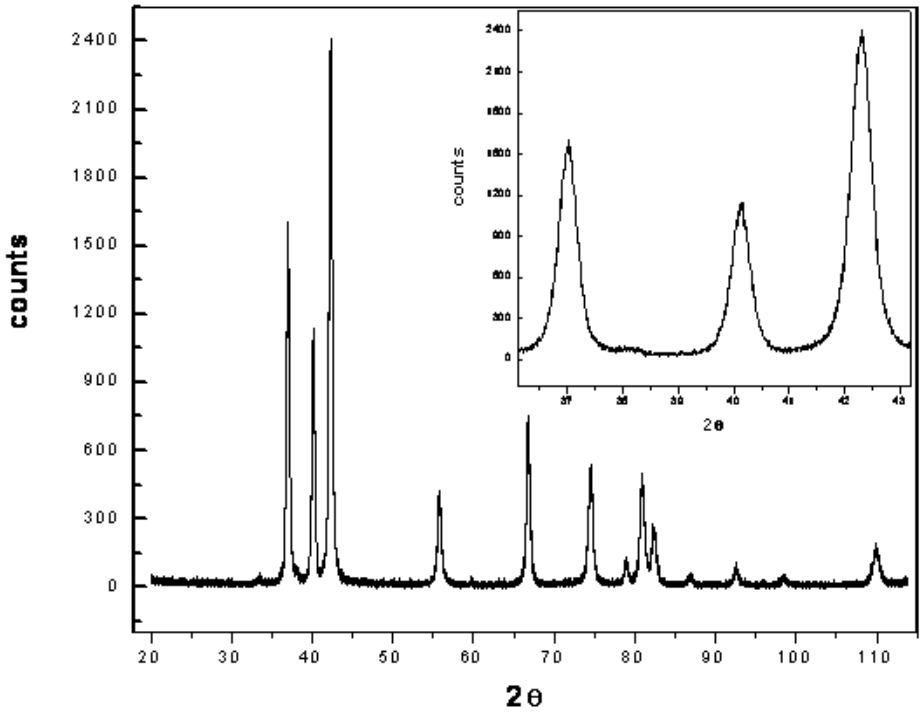

Fig. 1. XRD patterns of the synthesized ZnO powder.

(FWHM) and θ is the diffraction angle. The average size of ZnO crystallites was found to be 45nm.

The prepared ZnO powder was characterized by means of high resolution field–emission scanning electron microscopy (SEM) and energy dispersive X-ray (EDX) to explore surface morphology and composition, respectively. The SEM micrograph of figure 2 shows the morphology of a synthesized ZnO sample. As can be seen, the prepared ZnO contains very fine particles with an average size of about 50nm (Fig. 2a) which is in agreement with the XRD results. The EDX analysis was randomly performed on three different areas across the investigated sample to determine the zinc to oxygen ratio. As manifested in the EDX profile of figure 2b, only zinc and oxygen are detected indicating the high purity of the synthesized ZnO. Quantitatively the oxygen to zinc weight ratio was found to be approximately 1 to 4, respectively, indicating the stoichiometric formation of ZnO.

Nitrogen adsorption-desorption measurements were also carried out in order to determine the specific surface area of the synthesized ZnO. The prepared ZnO powder exhibits a specific surface area of 16.5 $m^2 g^{-1}$, determined by Brunauer-Emmett-Teller (BET) equation. Generally, the nanocrystalline materials should exhibit a high surface area. However, the relatively low surface area of the synthesized nanocrystalline ZnO might be attributable to agglomeration of clusters of nanoparticles.

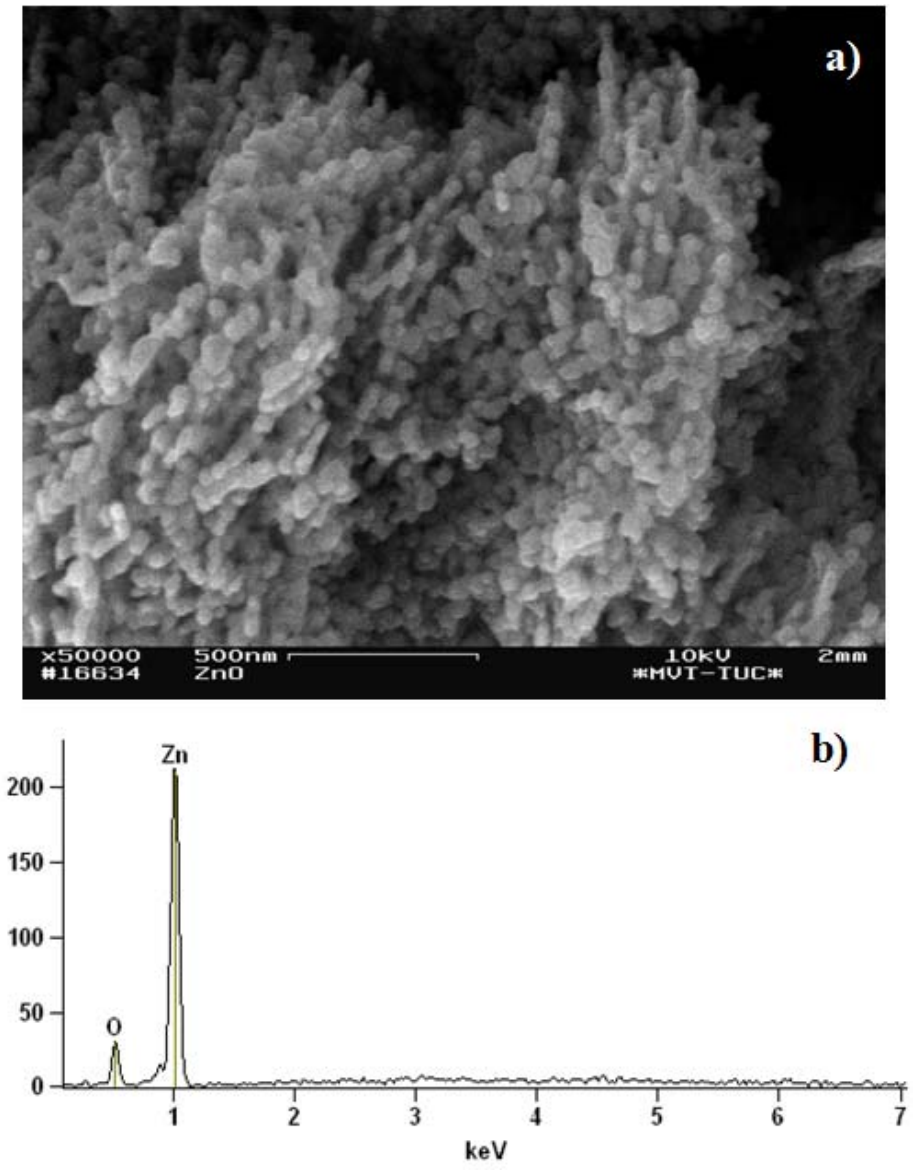

Fig. 2 SEM-EDX analysis of the prepared ZnO.

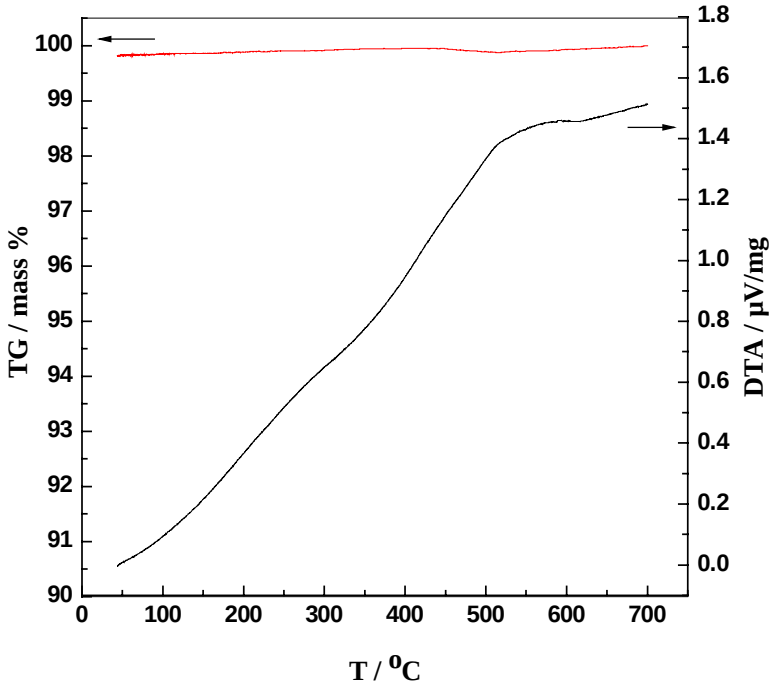

Fig. 3. DTA-TG curves of the prepared ZnO.

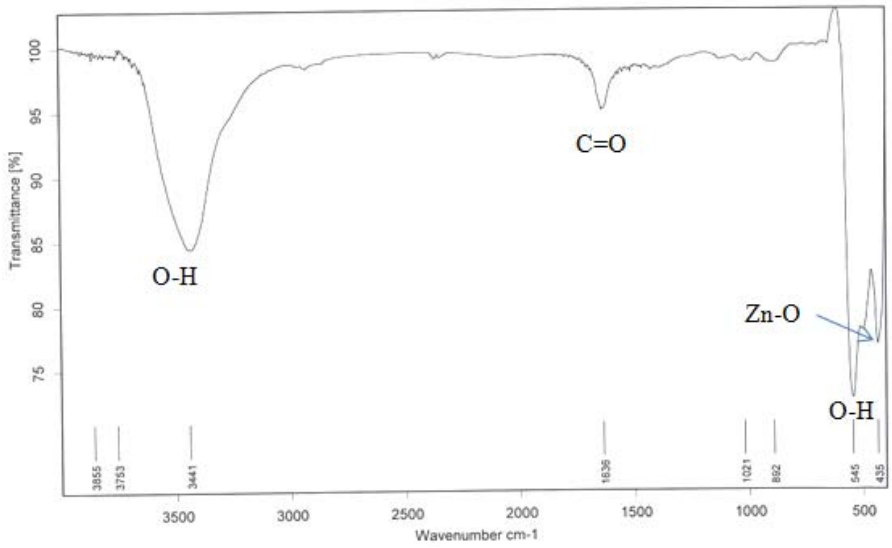

Fig. 4. IR spectrum of the prepared ZnO.

DTA-TG

The differential thermal analysis – thermogravimetric (DTA-TG) curves of the prepared ZnO are displayed in figure 3. It is clearly seen that the TG curve does not show any significant weight loss in the studied temperature range. This is not surprising as the sample was calcined at 450°C for 3hours. Therefore, the physically adsorbed water was totally evaporated. Furthermore, calcination has led to complete thermal transformation into ZnO. The DTA curve does not exhibit defined endothermic/exothermic peaks, however, an exothermic rise in the DTA curve is recorded from the

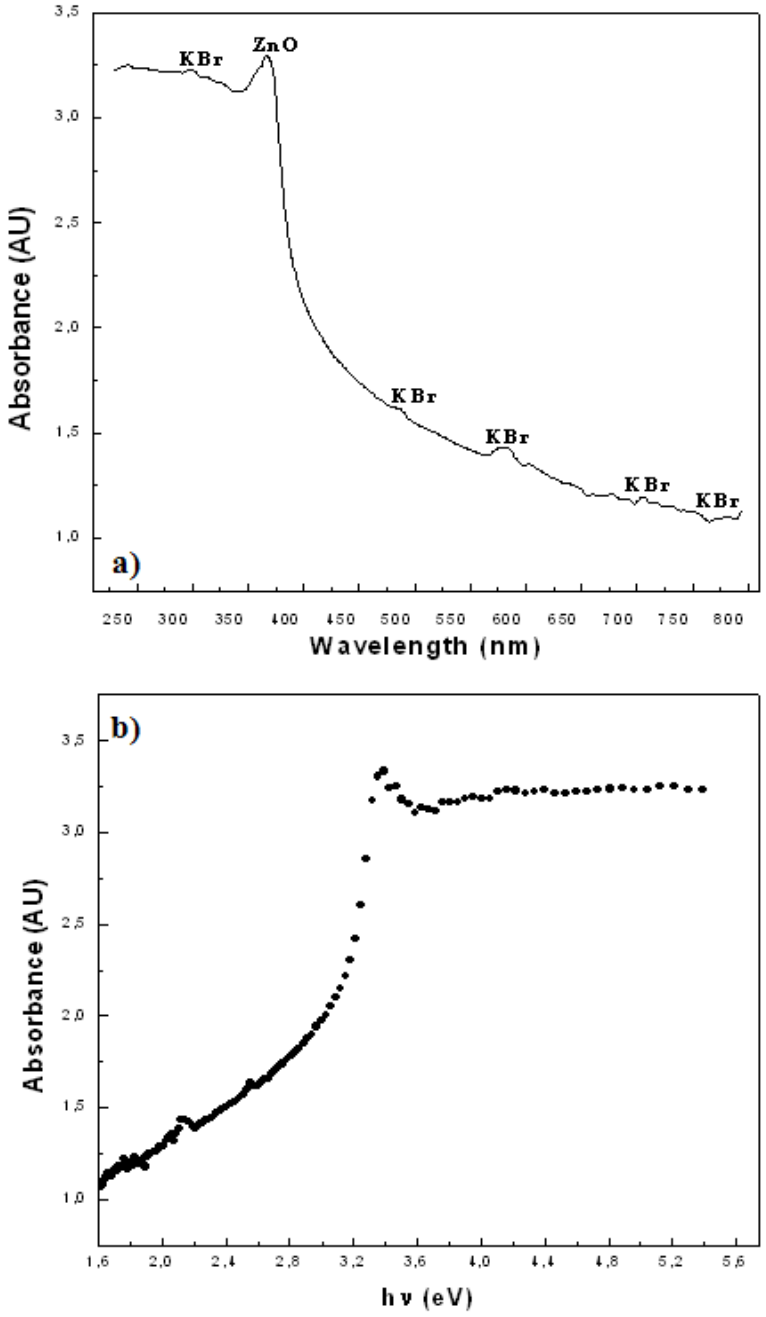

Fig. 5. UV-Visible spectrum of the prepared ZnO, a) absorbance vs. wavelength and b) absorbance vs. energy of the incident photon.

beginning up to 550 ^{o}C. This could be ascribed to the crystallization of the wurzite phase.

FT-IR Spectroscopy

The IR spectrum of the prepared ZnO powder is shown in figure 4. A significant absorption peak is observed at 3441 cm^{-1} as a result of O-H stretching vibrations. The peak observed at 1636 cm^{-1} is due to C=O stretching of carboxylate anions adsorbed on the surface of ZnO particles. The detection of such a peak indicates the difficulty of complete removing of the adsorbed carboxylate anions (from the zinc acetate precursor) even after extensive washing of the synthesized ZnO powder. The peak observed at 545 cm^{-1} is assigned to O-H

bending vibrations. Finally, the recorded peak at 435 cm^{-1} is ascribed to Zn-O stretching vibrations. The obtained IR results are consistent with literature data; see (Maensiri *et al*., 2006).

UV-Visible Spectroscopy

The band gap energy (E_g) is an important property of semiconductors as it determines their applications in electronics in general. In crystalline materials the (E_g) value is directly obtained from the absorption in the UV-visible region. The peak position of the absorption band of semiconductors can be well defined from the UV spectrum and hence, the band gap energy can be obtained. The UV-vis. absorption spectrum of the as-obtained ZnO powder is shown in figure 5a. Besides the standard weak peaks of KBr, the spectrum shows a significant absorption peak at 384 nm which is typical for ZnO (Shen, 2006). Figure 5b displays the absorption spectrum as a function of energy of the incident photon. The band gap energy (E_g) of the prepared ZnO powder was determined using the following equation:

$$\alpha (h\nu) = A (h\nu - E_g)^{m/2} \qquad (2)$$

where, α is the absorption coefficient, h is the Planck's constant, ν is the frequency of the incident photon and m = 1 represents a direct transition between valance and conduction bands. From the UV-vis. spectrum (Fig. 5b) the (E_g) was obtained by extrapolating a straight line from the absorption spectrum to the zero absorbance; $E_g = h\nu$ when α is zero. The results indicate a band gap of about 3.2 eV, showing a slight red shift compared to 3.37 eV for the bulk ZnO. This might be attributed to the agglomeration of ZnO particles.

CONCLUSIONS

In the present paper we have employed the direct precipitation method to synthesize nanocrystalline ZnO by using zinc acetate dihydrate as a precursor. Different microscopic and spectroscopic techniques were used to characterize the synthesized ZnO powder, SEM-EDX, XRD, IR, UV-vis., TG-DTA. The XRD results indicate that the synthesized ZnO has the wurtzite (hexagonal) structure with a crystallite size of about 45nm. The UV-vis. spectrum of the ZnO powder reveals a band gap of about 3.2 eV, showing a slight red shift. The prepared ZnO powder exhibits a specific surface area of 16.5 $m^2 g^{-1}$, determined by Brunauer-Emmett-Teller (BET) equation.

REFERENCES

Alivov, Ya.I., Kanilina, EV, Cherenkov, AE, Look, DC, Ataev, BM., Omaev, AK., Chukichev, MV. and Bagnall, DM. 2003. Fabrication and characterization of n-ZnO/p-AlGaN heterojunction light-emitting diodes on 6H-SiC substrates. Appl. Phys. Lett. 83: 4719-4721.

Bitenc, M., Marinsek, M. and Orel, ZC. 2008. Preparation and characterization of zinc hydroxide carbonate and porous zinc oxide particles. J. Eur. Ceram. Soc. 28**:**2915-2921.

Carotta, MC., Cervi, A., di Natale, V., Gheradi, S., Giberti, A., Guidi, V., Puzzovio, D., Vendemiati, B., Martinelli, G., Sacerdoti, M., Calestani, D., Zappettini, A., Zha, M. and Zanotti, L. 2009. ZnO gas sensors: A comparison between nanoparticles and nanotetrapods-based thick films. Sens. Actuators B. 137:164-169.

Carotta, MC., Guidi, AV., Malagù, C., Vendemiati, B. and Martinelli, G. 2005. Gas sensors based on semiconductor oxides: Basic aspects onto materials and working principles. Mater. Res. Soc. Symp. Proc. 828:173-184.

Deng, HM., Ding, J., Shi, Y., Liu XY. and Wang, J. 2001. Ultrafine zinc oxide powders prepared by precipitation/mechanical milling. J. Mater. Sci. 36:3273-3276.

Gao, YP., Sisk,CN. and Hope-Weeks, LJ. 2007. A sol-gel route to synthesis monolithic zinc oxide aerogels. Chem. Mater. 19:6007-6011.

Jiaquiang, X. Yuping, C., Yadong, L. and Jianian, S. 2005. Gas sensing properties of ZnO nanorodes prepared by hydrothermal method. J. Mater. Sci. 40:2919-2921.

Maensiri, S., Laokul, P. and Promarak, V. 2006. Synthesis and optical properties of nanocrystalline ZnO powders by a simple method using zinc acetate dihydrate and poly(vinyl pyrrolidone). J. Cryst. Growth 289:102-106.

Martins, R., Fortunato, E., Nunes, P., Ferreira, I., Marques, A., Bender, M., Katsarakis, N., Cimalla, V. and Kiriakidis, G. 2004. Zinc oxide as an ozone sensor. J. Appl. Phys. 96:1398-1408.

Music, S., Dragcevic, D., Maljkovic, M. and Popovic, S. 2002. Influence of chemical synthesis on the crystallization and properties of zinc oxide. Mater. Chem. Phys. 77**:**521-530.

Nyffenegger, RM., Craft, B., Shaaban, M., Gorer, S., Erley, G. and Penner, RM. 1998. A hybrid electrochemical/chemical synthesis of zinc oxide nanoparticles and optically intrinsic thin films. Chem. Mater.10:1120-1129.

Rani, S., Suri, P., Shishodia, PK. and Mehra, RM. 2008. Solar Energy Mater. & Solar Cells. Synthesis of nanocrystalline ZnO powder via sol-gel route for dye-sensitized solar cells. 92:1639-1645.

Redmond, G., Fitzmaurice, D. and Graetzel, M. 1994. Visible-light sensitization by cis-bis(thiocyanato)bis(2,2-bipyridyl-4,4-dicarboxylato)ruthenium(II) of a transparent nanocystalline ZnO film prepared by sol-gel techniques. Chem. Mater. 6:686-691.

Scherrer, P. 1918. The Scherrer Formula for X-Ray Particle Size Determination. Göttinger Nachrichten. 2:98-100.

Shen, L., Bao, N., Yanagisawa, K., Domen, K., Gupta, A. and Grimes, CA. 2006. Direct synthesis of ZnO nanoparticles by a solution-free mechanochemical reaction. Nanotechnology. 17:5117-5123.

Sigoli, FA., Davolos, MR. and Jafelicci Jr., M. 1997. Morphological evolution of zinc oxide originating from zinc hydroxide carbonate. J. Alloys Comp. 262-263:292-295.

Wang, HT., Kang, BS., Ren, F., Tien, LC., Sadik, PW., Norton, DP., Pearton, SJ. and Lin, J. 2005. Hydrogen-selective sensing at room temperature with ZnO nanorods. App. Phys. Lett. 86:243503.

Xu, HY., Wang, H., Zhang, YC., He, WL., Zhu, MK., Wang, B. and Yan, H. 2004. Hydrothermal synthesis of zinc oxide powders with controllable morphology. Ceram. Inter. 30:93-97.

Received: July 9, 2010; Accepted: Aug 26, 2010